CONSTITUTIVE GRADIENTS AND PORE TOLERANCE IN TWO WELDMENTS

Brad L. Boyce (blboyce@sandia.gov), Charles V. Robino, and Phillip L. Reu
Sandia National Laboratories, Albuquerque, New Mexico

SAND2006-7098P

Sandia National Laboratories

Introduction

The constitutive stress-strain behavior **of small scale welds, such as produced by laser welding, is difficult to evaluate using conventional methods. To address this issue, a digital image correlation (DIC) technique was applied to map the strain inhomogeneities around transverse laser welds. The strain map was used to (a) characterize gradients in stress-strain material behavior, and (b) assess the origins of failure, i.e. to evaluate the role of weld-root porosity on structural integrity.**

Method

Digital Image Correlation (DIC)

enables a direct spatial mapping of the in-plane components (2D) of strain, ε_{xx}, ε_{yy}, and ε_{xy} [P. Cheng *et. al*, *Exp. Mech.*, 2002]. A bead-blasted surface provided the necessary speckle patterns (Fig. 1). Tensile tests were performed on transversely welded tensile coupons that were planarized to produce a geometrically rectangular tensile bar (Fig. 2).

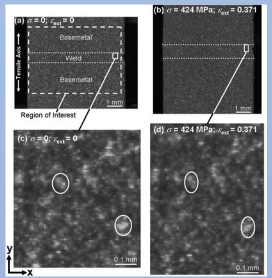

Fig. 1. Before (left) and After (right) speckle patterns used for digital image correlation.

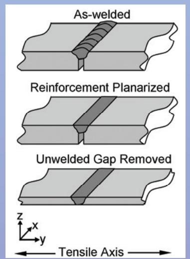

Fig. 2. Transverse laser welds were planarized to create geometrically rectangular tensile bars with a nominally homogeneous stress-field

Tensile Test Material & Conditions

304L Laser Weld:

- -304L Austenitic Stainless Steel, 1.6 mm thick sheet.
- -Laser Welded with Continuous (CW) or Pulsed Wave (PW)
- -Partial penetration butt welds (depth ~0.5 mm, ~30% pen.)
- -Welded sheet planarized to remove unwelded gap.
- -Tensile bar was bead blasted to produce image speckles.
- -Nominal strain rate of 7×10^{-4} s^{-1}.
- -Gage width = 6.35 mm. Extensometer gage length = 12.7 mm.
- -1392x1040 pixel digital camera used to capture speckle field.

Ni-Cr-Mo-Gd GTAW Weld:

- -Neutron-Absorber Alloy (UNS N06464 in ASTM std. B932-04)
- -Welded with automated pulsed Gas Tungsten Arc Weld
- -25He/75Ar shielding gas and Gd-free Ni-Cr-Mo filler metal
- -Full-penetration weld in 9.52 mm thick plate
- -Similar DIC technique, applied to weld cross-section

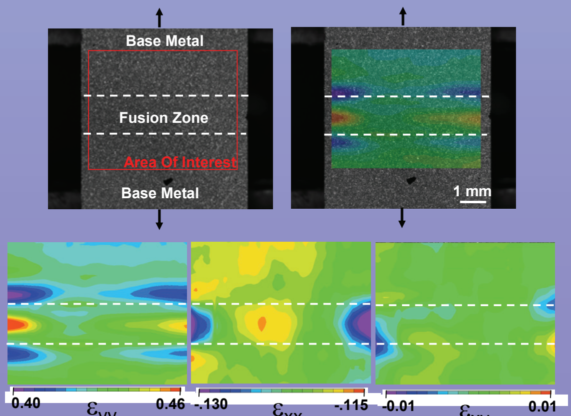

Fig. 3. Example of a speckled laser welded tensile bar and corresponding DIC maps of in-plane strain components. This particular example was a continuous-wave (CW) weld loaded at a stress of 616 MPa (near the ultimate strength). The tensile axis is the y-axis.

Constitutive Gradients

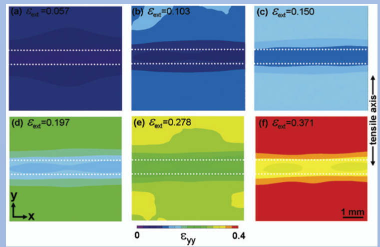

Fig. 4. Maps of strain along the tensile axis, ε_{yy}, showing suppressed strain in the vicinity of the weldment (delineated by white dotted lines). [PW condition, qualitatively similar to CW cond.]

Spatial Strain Maps such as shown in Fig. 4, revealed tha the fusion zone was harder (less strain) than the neighboring basemetal, with a smooth strain gradient between the two regions. Stress-strain curves were extracted from the center of the fusion zone and basemetal, providing a direct quantitative measure of the difference in constitutive properties between the two regions, which can now be embedded in high-fidelity structural models of welded components.

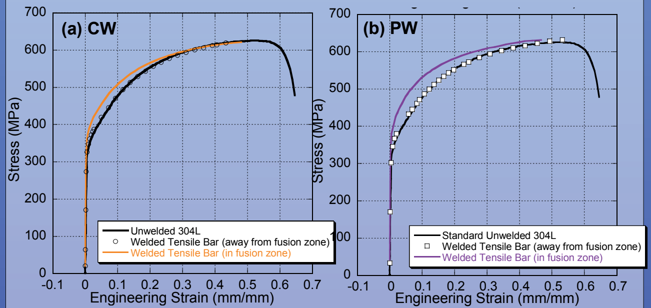

Fig. 5. DIC-measured stress-strain curves extracted from the center of the fusion zone and from the basemetal far from the weldment, as compared to a conventional tensile test on unwelded 304L. Notice the fusion zones are slightly harder than the basemetal.

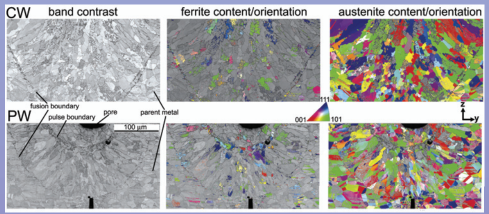

Fig. 6. Microstructural differences in the fusion zones from the two conditions.

Table 1. Strengthening of the weldments was attributed primarily to differences in the ferrite content and grain size.

Laser Welding Process	Estimated Hall-Petch Strengthening in Fusion Zone (MPa)	Estimated Ferrite Strengthening in Fusion Zone (MPa)	Sum of Hall-Petch and Ferrite Strengthening (MPa)	Actual Observed Strengthening in Fusion Zone (MPa)
Continuous Wave (CW)	9-17	12-16	21-33	~40
Pulsed Wave (PW)	32-59	20-26	52-85	~70

Conclusions

Observed fusion-zone strengthening (Fig. 5) was largely attributed to grain-size (Hall-Petch) and ferrite content differences between the basemetal and the fusion zone (Fig. 6 and Table 1).

For More Information: B.L. Boyce, P.L. Reu, and C.V. Robino, "The Constitutive Behavior of Laser Welds in 304L Stainless Steel Determined by Digital Image Correlation", Metallurgical and Materials Transactions A, vol. 37A, p. 2481-2491, 2006.

Pore Tolerance

Example: 304L Stainless Steel As shown in Fig. 7, the pulsed wave (PW) condition contained a signficant fraction of large weld-root pores, whereas in the continous wave (CW) condition, the pores were limited or non-existent. However, as shown in Fig. 5, there was no notable degradation in either the ductility or the strength in the pore-containing PW condition compared to the CW condition. This pore tolerance is thought to be due to the extensive ductility (>50% elongation) available to accommodate flaws in the 304L alloy.

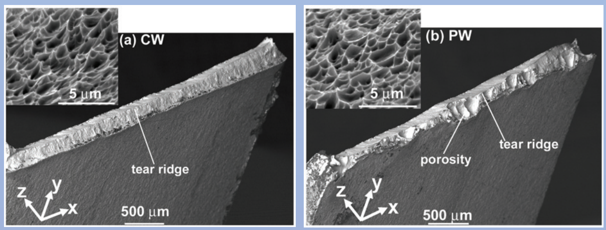

Fig. 7. In the observed tensile fracture surfaces, it is apparent that the pulsed wave (PW) condition had substantial weld root porosity, whereas the continuous wave (CW) condition had little or no porosity.

Counter-Example: Ni-Cr-Mo-Gd Ferrous Alloy The fusion zone of this alloy is much less ductile than 304L. Even after a post-weld heat-treatment, the alloy only exhibits 11-13% elongation at failure. In this case, when pores are found in the weldment (Fig. 9), strain localizes at the pore and failure occurs at low macroscopic strains <1% (Fig. 8). Interestingly, the DIC method revealed that the local strain at failure (Fig. 9), was roughly similar to the materials' macroscopic ductility (i.e. in the simplest sense, the pore concentrated strain until a local strain failure criterion was reached).

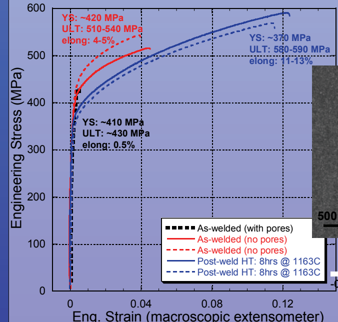

Fig. 8. Differences in ductility and strength for a weld with pores compared to a pore-free weld and a pore-free heat treated weld. When pores were present, the weld failed at very low macroscopic strain <1%.

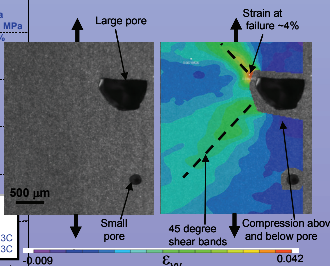

Fig. 9. Strain map in the vicinity of two pores taken immediately prior to catastropic failure. Note that the local maximum strain value was 4%, similar to the macroscopic ductility of the as-welded material without pores.

Conclusions

The high-ductility 304L alloy showed no degradation due to porosity (Figs. 5 and 7), whereas the much less ductile Ni-Cr-Mo-Gd alloy was intolerant of the pore flaws, and localized strains at the pores exceeded the material's ductility, leading to premature failure.

Acknowledgements: The authors would like to thank J. R. Michael, F. Hooper, T. Crenshaw, and A. Kilgo. Sandia is a multiprogram laboratory operated by Sandia Corporation, a Lockheed Martin Company, for the United States Department of Energy's National Nuclear Security Administration under contract DE-AC04-94AL85000.